Atmospheric Research 138 (2014) 13–29

Contents lists available at ScienceDirect

Atmospheric Research

journal homepage: www.elsevier.com/locate/atmos

Analysis and hindcast simulations of an extreme rainfall event in the Mediterranean area: The Genoa 2011 case

E. Fiori [a,*], A. Comellas [a,c], L. Molini [a], N. Rebora [a], F. Siccardi [a,c], D.J. Gochis [d], S. Tanelli [b], A. Parodi [a]

[a] CIMA Research Foundation, Savona, Italy
[b] Jet Propulsion Laboratory, California Institute of Technology, Pasadena, CA, United States
[c] University of Genoa, Italy
[d] National Center for Atmospheric Research, Boulder, CO, United States

ARTICLE INFO

Article history:
Received 3 June 2013
Received in revised form 23 September 2013
Accepted 8 October 2013

Keywords:
Deep convection
Numerical modeling
Flash flood

ABSTRACT

The city of Genoa, which places between the Tyrrhenian Sea and the Apennine mountains (Liguria, Italy) was rocked by severe flash floods on the 4th of November, 2011. Nearly 500 mm of rain, a third of the average annual rainfall, fell in six hours. Six people perished and millions of Euros in damages occurred. The synoptic-scale meteorological system moved across the Atlantic Ocean and into the Mediterranean generating floods that killed 5 people in Southern France, before moving over the Ligurian Sea and Genoa producing the extreme event studied here.

Cloud-permitting simulations (1 km) of the finger-like convective system responsible for the torrential event over Genoa have been performed using Advanced Research Weather and Forecasting Model (ARW-WRF, version 3.3).

Two different microphysics (WSM6 and Thompson) as well as three different convection closures (explicit, Kain–Fritsch, and Betts–Miller–Janjic) were evaluated to gain a deeper understanding of the physical processes underlying the observed heavy rain event and the model's capability to predict, in hindcast mode, its structure and evolution. The impact of forecast initialization and of model vertical discretization on hindcast results is also examined.

Comparison between model hindcasts and observed fields provided by raingauge data, satellite data, and radar data show that this particular event is strongly sensitive to the details of the mesoscale initialization despite being evolved from a relatively large scale weather system. Only meso-γ details of the event were not well captured by the best setting of the ARW-WRF model and so peak hourly rainfalls were not exceptionally well reproduced. The results also show that specification of microphysical parameters suitable to these events have a positive impact on the prediction of heavy precipitation intensity values.

1. Introduction

Floods are the most dangerous meteorological hazard in the Mediterranean due to both the number of people affected and to the relatively high frequency by which human activities and goods suffer damages and losses (Llasat-Botija et al., 2007). These facts are evidenced by the noteworthiness of several historical disastrous events that have been previously studied including; the 1970 Genoa case (northern Italy) studied by Roth et al. (1996) and Siccardi (1996) among others, the 1992 Vaison-la-Romaine event (southern France; Massacand et al., 1998; Ducrocq et al., 2008), the Izmir case (west Turkey) in 1995 (Komuscu et al., 1998), and the disastrous flash flood of Bab-el-Oued in 2001 (Argence et al., 2008; Branković et al., 2008; Tripoli et al., 2005).

* Corresponding author.
E-mail address: elisabetta.fiori@cimafoundation.org (E. Fiori).

0169-8095
http://dx.doi.org/10.1016/j.atmosres.2013.10.007

Despite its generally mild climate, severe weather events are a significant part of the Mediterranean climate on both northern and southern shores. It is not uncommon to observe that the rain accumulated in one hour accounts for an entire monthly average for that location, and the rain accumulated in one day accounts for the entire yearly average (Altinbilek et al., 1997). Additionally, Barredo (2007) found that in the period 1950–2005 up to 40% of casualties have been due to flash-floods, related, at least in part, to the growing population and the expanding economic development in the region. These impacts are only expected to increase in the coming decades. Also shown in Barredo (2007), half of the major flood events from 1950 to 2005 in the European Union mainly took place in Italy, Spain and southern France causing more than 2750 fatalities with an average rate of about 50 per year. Lastly, it is now widely expected that climate change will increase the occurrence of severe rainfall events in many regions around the world including the Mediterranean (Groisman et al., 2004, 2005).

The principal meteorological pre-conditions or 'ingredients' for potentially disastrous flash floods are quite well known and were summarized by Delrieu et al. (2005). First, a deep and sustained source of heat and moisture is required and is often provided by the Mediterranean Sea in September up to mid-November as it cools from its late-summer peak heat content. The second ingredient is the convergence and lifting provided by synoptic configurations which, in the case of many Mediterranean storms, are dominated by extended troughs that advect south (easterly or westerly) flow to the coasts. The third driving factor is the presence of significant orography next to the sea which can amplify and focus low-level moisture convergence and trigger deep convective motion within the flow (Altinbilek et al., 1997).

Very often the structures responsible for these kinds of events are quasi-stationary meso-β convective systems. In such cases it is not uncommon for intense, though often small-sized, storms to repeatedly impact the same area for several hours. In essence, new convective cells continually regenerate at approximately the same rate at which the older ones are advected away (Chappell, 1986). Regional radar and satellite imagery frequently reveal these stationary or backward regenerative systems that assume a characteristic V-shape (Delrieu et al., 2005).

The severity of these events can be tightly dependent on local factors such as upwind islands, complex coastlines and steep orography, so that even very small scale (e.g., a few kilometers) features need to be considered. To improve prediction capabilities progress must be made in understanding the mechanisms that govern the precise location of the precipitation system as well as of those that can occasionally produce uncommon amounts of precipitation (Ricard et al., 2012).

With this aim, this paper is devoted to the study of the extreme rainfall event that took place in Genoa on November 4th, 2011, by means of high-resolution numerical simulations and observational data analysis.

The original idea of numerical prediction of severe rainfall events, associated with deep moist convective processes, dates back to the fundamental studies of Lilly (1990) and Droegemeier (1997), which described possible approaches and challenges to develop numerical prediction of convective storms. Since then, many studies have demonstrated the importance of convective-scale numerical weather models (Xue et al., 2007; Done et al., 2004; Kain et al., 2006; Roberts and Lean, 2008) for research and early-warning activities. At the same time, advances in quantity, quality, and resolution of available observational data and in high-performance computing (HPC) (Xue et al., 2007) promote the use and validation of increasingly more sophisticated and computationally demanding atmospheric models.

However, many sources of uncertainty still exist and continue to play a crucial role in forecasting precipitation rate and distribution. Among them, the choices of the horizontal resolution and the associated choices of physics parameterizations for unresolved sub-grid scale processes remain as important modeling decisions (Yu and Lee, 2010). Severe weather scenarios associated with land-falling Mediterranean storms are natural laboratories for exploring high-impact hydro-meteorological events and their correlated uncertainty sources. By incorporating high-quality observational data there exists significant potential to improve modeling and prediction capabilities, to identify the root causes of such events, and to improve detection and management of those threatening phenomena (Borga et al., 2007; Delrieu et al., 2005; Llasat et al., 2003).

Specifically, in this paper, the performance of a cloud-permitting (1 km) model is assessed by the analysis of different sets of numerical simulations of the convective system responsible for the catastrophic event of November 2011 in the Liguria region. Our focus is to evaluate the sensitivity of the Advanced Research Weather and Forecasting Model (ARW-WRF, version 3.3) by the specification of cloud microphysics and methods for cumulus parameterization as well as to other model decisions such as initialization conditions and vertical model discretizations. Thus, a set of simulations combining two different microphysics (WSM6 and Thompson, described in Section 3 below) and three different cumulus convection approaches (explicit, Kain–Fritsch, and Betts–Miller–Janjic) were executed to gain a deeper understanding of the kinematic and thermodynamical processes underlying the event. The comparison of modeling findings with a host of observed meteorological fields provided by raingauge, satellite and radar data is provided. The final goal is to offer the evaluation and justification for optimal configurations of the model focused on defining a highly dependable suite for the use in ongoing forecasting operations. Section 2 provides a description of the meteorological scenario; Section 3 details the specifics of the model experiment configurations and the data used to initialize and evaluate the model; Section 4 addresses the analysis of the modeling results, and Section 5 provides some discussion and final considerations.

2. The severe weather scenario

The synoptic-scale meteorological system responsible for the Genoa flash flood event originated days before from western Atlantic Ocean and moved into the Mediterranean, where the storm re-intensified significantly due, in part, to the moisture inflow provided by an anomalously warm western Mediterranean Sea. In particular, a positive anomaly of temperature was observed in the central part of the Ligurian Sea (Rebora et al., 2013). Finally, on the 4th and 5th of November, extreme rainfall hit Provence (Southern France) and Liguria

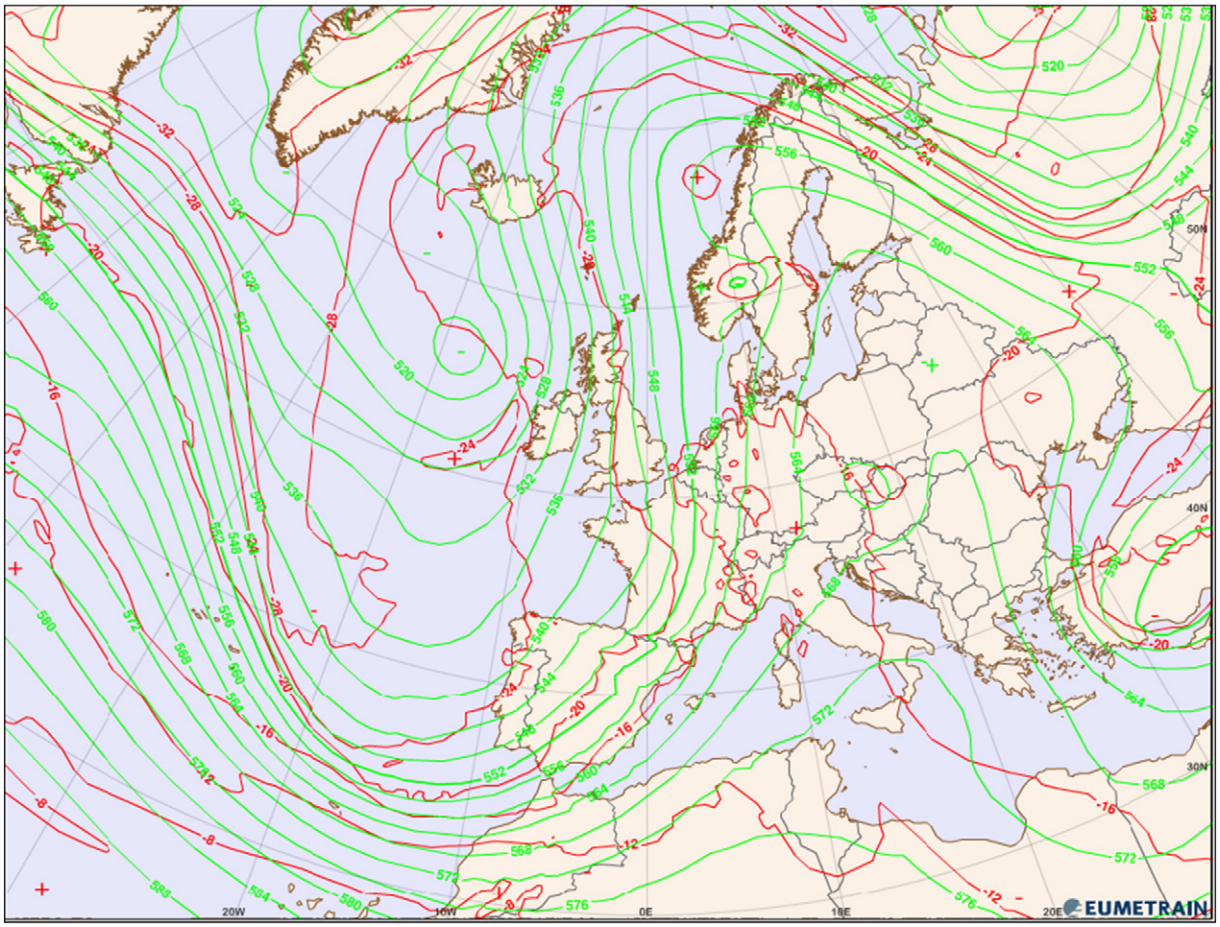

Fig. 1. 500 hPa analysis map at 00UTC on November 4th 2011 (ECMWF model run on November 4th 2011 at 00 UTC): temperature in red (°C) and geopotential height in green (gpm).

(North-Western Italy), killing 5 and 6 people in the respective areas (Parodi et al., 2012; Rebora et al., 2013).

Fig. 1 shows the 500 hPa height analysis at 00 UTC on November 4th, 2011 (GFS model run initialized at 00UTC on November 4th, 2011), a few hours before the heavy precipitation period over Liguria. An upper-level low centered northwest of Ireland extended southward to the Iberian Peninsula, resulting in mid-level southwesterly flow over the Ligurian Apennine Mountains. At low elevations (around 850 hPa) the flow was primarily southeasterly. This synoptic setting supported pronounced moist air advection and precipitation from the sub-tropical Mediterranean areas near North Africa (Fig. 2). The high water vapor contents along the storm track and into the system were further enhanced by the recurvature of the remnants of the Tropical Cyclone Rina (October 23rd–28th over the western Caribbean sea) (not shown).

Based on the approach discussed in Molini et al. (2011) and as shown below, this kind of storm system can be classified as a "convective-equilibrium" case. This means that the production of CAPE by large-scale processes is nearly balanced by its consumption within convective phenomena. Correspondingly, local CAPE values remain small and CIN is negligible. The time-scales of convective processes are typically small (i.e. minutes to less than one hour) compared with the time-scales of larger-scale forcing changes (typically several hours) and, consequently, convection may be considered to be in a state of statistical equilibrium with the larger scale forcing. This situation is supported by the skew-T diagrams of six radiosonde sounding stations (Barcelona, Palma de Mallorca, Nimes, Cagliari, Ajaccio and Milano) located under or near the frontal system at 00 UTC on 4th November 2011: maximum measured CAPE was 500–600 J/kg and CIN values were slightly negative (Fig. 3).

All the characteristic synoptic and mesoscale environmental conditions that usually lead to heavy convective precipitation events over complex orography regions (Doswell et al., 1998; Lin et al., 2001; Miglietta and Rotunno, 2010) were present:

i) conditionally or potentially unstable air masses, as observed by the aforementioned radiosounding values;
ii) moist low-level jets that impinge the first foothills, as confirmed by the southeasterly flow at 850 and 700 hPa;
iii) steep orography (the Apennines ridge with elevation up to 1500 m in 10–20 km from the coastline) which helps to release the conditional instability associated with the low-level jet;
iv) slowly-evolving synoptic pattern that inhibits rapid

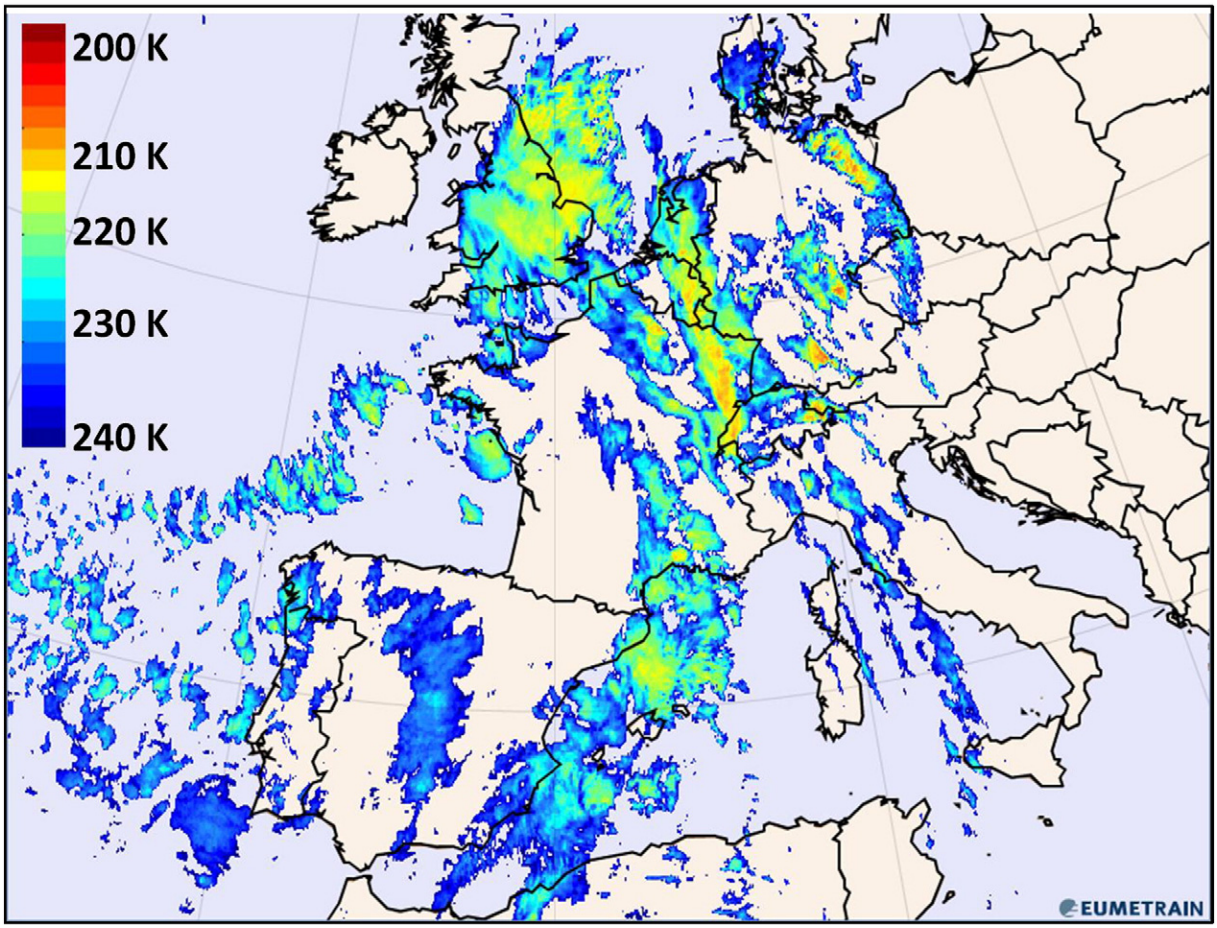

Fig. 2. Meteosat Second Generation (MSG)—Infrared image, showing cloud top temperature image at 00UTC, 4th November 2011 (from www.eumetrain.org).

movement of the heavy precipitation system or maintains the same favorable local environment for intense precipitation (note the blocking conditions due to a strong pressure ridge centered on eastern Europe as visible in Fig. 1).

The combination of these ingredients resulted in the torrential rainfall event observed in Genoa. Specifically, a v-shaped, isolated and self-regenerating mesoscale convective system (MCS), as observed by the Italian radar network composite (Fig. 4), was triggered over the Gulf of Genoa on the night of 4th November (01UTC ÷ 02UTC). The cell then moved slowly towards the west along the eastern coast of Liguria region from approximately 03UTC to 09UTC (Fig. 4) and finally locked over the western portions of the Genoa hills where it produced intense convective activity (Rebora et al., 2013) and extreme rainfall depth. The persistence of this rainfall event over the central-eastern portion of the Liguria region between 09UTC and 15 UTC is confirmed by the values of precipitation radar reflectivity. Over the impact area the reflectivity was above a 40 dB threshold (Rebora et al., 2013) for more than four hours. This persistence appears to have been driven by local convergence as suggested by Moncrieff and Liu (1999) and Wang et al. (2000). The Advanced Scatterometer (ASCAT) Ocean Surface Wind Vectors data image (25 km in resolution) referred at 9:30 UTC (Fig. 5) shows through low-level wind bar a mesoscale convergence line where cold air coming from north-northwest collided with warm and moist air coming from the southeast over the Liguria region.

The convective cell generated under these atmospheric conditions was aligned in a southwest–northeast axis, along the direction of maximum slope of the orography in eastern Liguria, thereby promoting the efficiency of the orographic precipitation mechanisms. These features are in good agreement with Boni et al. (2008) who studied similar systems in the Ligurian region.

Ground observations of rainfall between 09 UTC and 15 UTC (upper panel of Fig. 6) were measured by the Italian Civil Protection Department (ICPD) raingauge network, which has an average spatial density of one gauge every 75 km^2. Stations located in the Genoa city center measured up to about 500 mm in 6 h, a depth with a return period in excess of 200 years (Boni et al., 2006).

3. Numerical model setup

The Advanced Research Weather Research and Forecasting (ARW-WRF), version 3.3 is a fully compressible, 3D, Eulerian, nonhydrostatic regional atmospherical model. For a

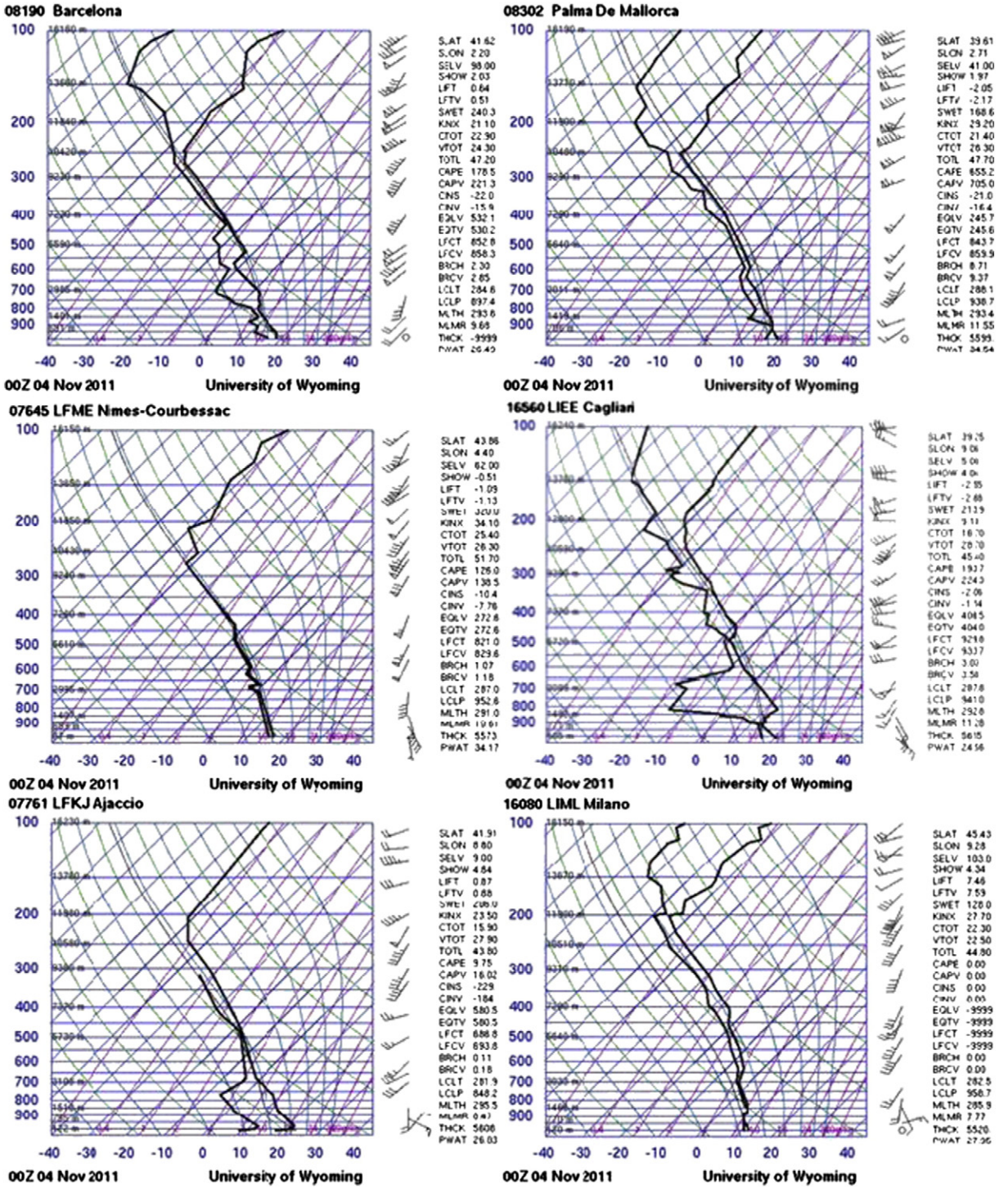

Fig. 3. skew-T diagrams at 00UTC, 4th November 2011, for Barcelona, Palma de Maiorca, Nimes, Cagliari, Ajaccio, and Milano Linate (courtesy of University of Wyoming, Department of Atmospheric Science). The two bold black lines represent the dew-point (on the left) and the temperature vertical profile. The purple lines are mixing-ratio lines. The green lines are dry adiabat lines. The blue curved lines are wet adiabat lines. The barbs on the right side of the skew-T show how fast the wind is travelling. The part of the flag with the barbs points to the direction the wind is coming from. The end point (pointy section) points to the direction the wind is travelling to. Half a barb stands for 5 kn, a full barb stands for 10 kn, and a bold barb stands for 50 kn.

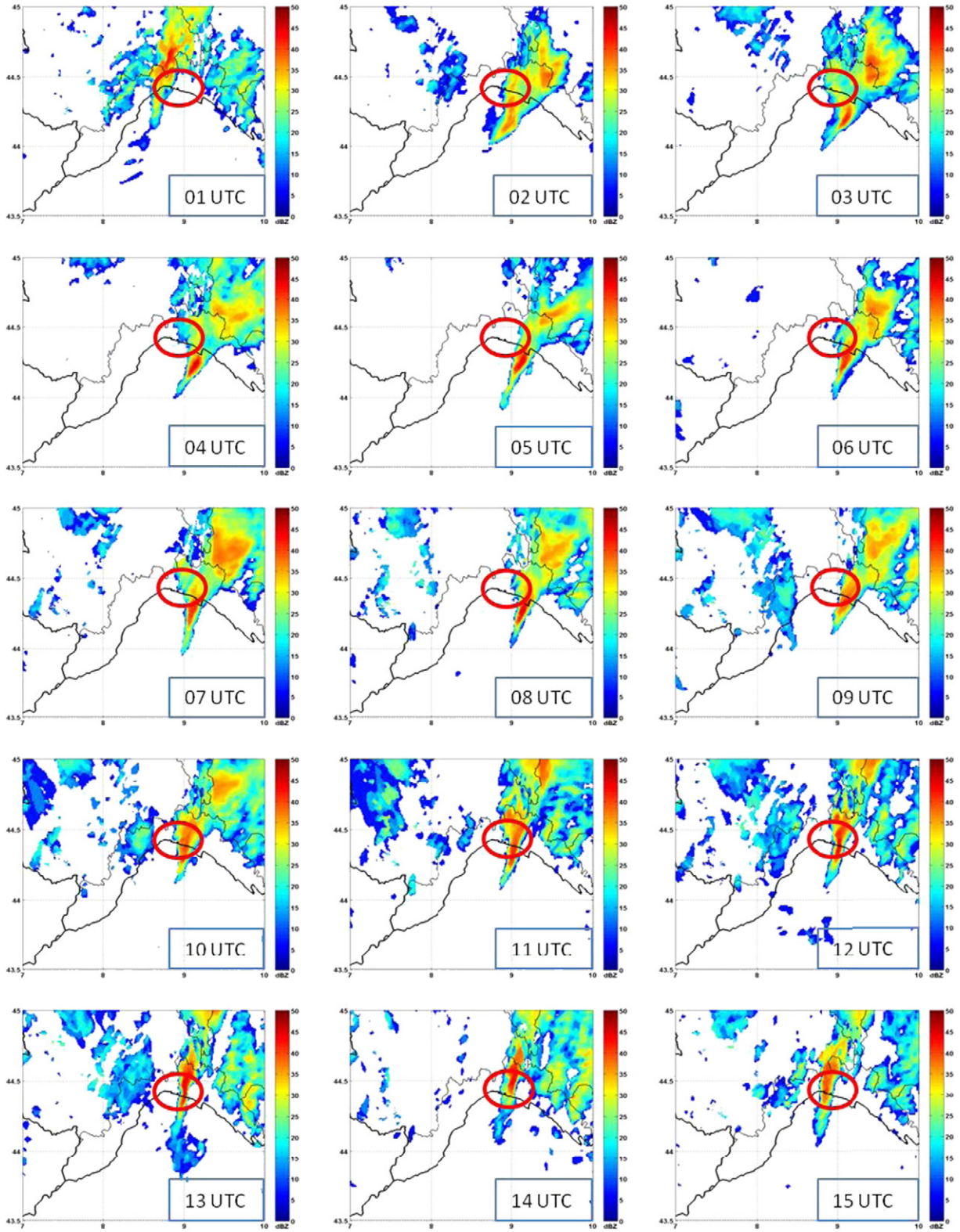

Fig. 4. Reflectivity on a Constant Altitude Plan Position Indicator (CAPPI) [dBZ] at 2000 m (from 01UTC to 15UTC, 04/11/2011) as provided by the Italian radar network composite. The red ellipsoid highlights the target area for this study corresponding to the Genoa city.

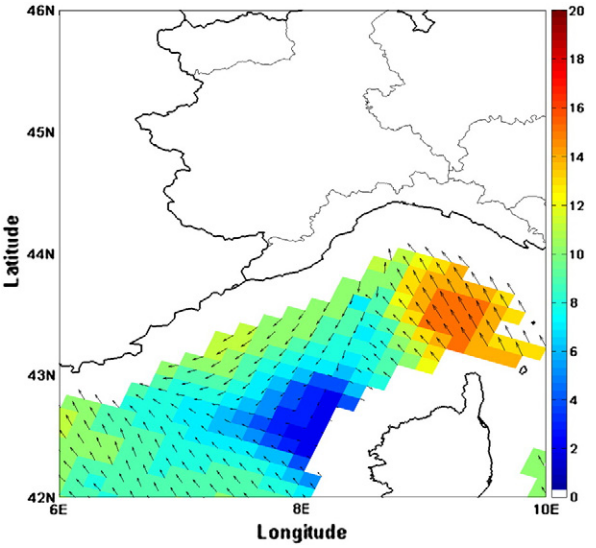

Fig. 5. Advanced Scatterometer (ASCAT) ocean surface wind vectors data of 25 km resolution, on 4th November 2011, descending pass (10 UTC). The black dashed line identifies the low-level convergence zone of the wind field over the ocean.

comprehensive description of this model, the reader is referred to Skamarock et al. (2005).

Two nested domains (d_1 and d_2 at 5 and 1 km grid spacing, respectively) (Fig. 7) cover the upper and lower limits of the cloud-permitting range (Arakawa, 2004). In the first set of simulations, the vertical coordinate was discretized in 28 levels, equally spaced in hydrostatic pressure coordinates with 8 levels in the lowest 2.5 km. The enhanced number of layers near the surface was intended to help in resolving the complex flow over the coastal orography and its associated convective activity. Additional model experiments were run to evaluate the sensitivity of the model results with respect to the number of vertical layers.

Ten model configurations are chosen as summarized in Table 1. From a microphysical point of view, two different moment or 'bulk' microphysics parameterizations were chosen: the WRF Single-Moment 6-Class Scheme (WSM6, Hong and Lim, 2006) and the Double-Moment Thompson et al. (2004) scheme. The WSM6 scheme extends the WSM5 scheme to include graupel and its associated microphysical processes. Some of the graupel-related terms follow Lin et al. (1983), but its ice-phase behavior is very different due to the changes of Hong et al. (2004). Mixed-phase snow and graupel particles are assigned a single fall-speed weighted by the mixing ratios, which is applied to both sedimentation and accretion processes (Dudhia et al., 2008).

The Thompson scheme, compared to earlier single-moment approaches, incorporates a large number of improvements to both physical processes and computational methods and, additionally, employs several techniques found in more sophisticated spectral/bin microphysics schemes. The assumed snow size distribution depends on both ice water content and temperature and is represented as a sum of exponential and gamma distributions. Furthermore, snow assumes a non-spherical shape with a bulk density that varies inversely with diameter as found in observations (Thompson et al., 2004, 2008).

The choice to use these two microphysical parameterizations which involved all 6 hydrometeors was driven from the fact it was noted that during its most intense phase, the convective cell observed in the Genoa event exhibited a fairly deep cloud top composed of small ice particles and corresponding roughly to a height of 10–12 km (Rebora et al., 2013).

The grid spacing ranges between 5 and 1 km, corresponding to d_1 and d_2 domains respectively, should make the model able to resolve explicitly, albeit crudely, many convective processes (Kain et al., 2006, 2008). More studies have investigated numerical simulations at the so-called "grey-zone" resolution (Gerard, 2007) to understand if convective parameterization is still able to work correctly on those scales. It is still an open question (Yu and Lee, 2010).

The peculiar fine-grained features of the self-regenerating convective cell described above motivated a joint investigation of explicit and non-explicit CPM model settings, described hereafter in detail. Building on those earlier efforts this study evaluates three different cumulus convection approaches:

i) explicit method: no sub-grid closure formulation is used;
ii) Betts–Miller–Janjic: profile relaxation type scheme (Betts, 1986; Betts and Miller, 1986);
iii) Kain–Fritsch: mass-flux type scheme (Kain and Fritsch, 1990).

The Betts–Miller–Janjic scheme adjusts the sounding toward a pre-determined, post-convective reference profile derived from climatology. This scheme works well in moist environments with little convective inhibition; it is the most effective scheme at preventing the microphysics scheme from trying to create convection (Gallus, 1999), and implicitly includes the cloud layer effects of downdrafts, latent heat of condensation and fusion from phase changes in updrafts, melting of falling precipitation, and many other complicated natural features. Known shortcomings of the Betts–Miller–Janjic scheme are that reference profiles are fixed based on climatological observations rather than being flexible for actual, evolving environmental conditions. It is only triggered for soundings with deep moisture profiles, and when triggered, the scheme often consumes available humidity too quickly, either because the reference profile is too dry for the forecast situation or because the transition to the reference profile is too rapid. This leaves too little water vapor behind for precipitation to occur later or downstream (Jankov et al., 2005).

The Kain–Fritsch parameterization is a mass-flux scheme designed to rearrange mass in a column so that CAPE is consumed. Its assumption about consumption of CAPE is appropriate for short time and space scales and it accounts for microphysical processes in convection. Furthermore, the scheme offers a plausible treatment of convection triggering and convective inhibition. However, it may tend to leave unrealistically deep saturated layers in post-convective soundings, causing in turn the microphysics scheme to be activated and to over-simulate post-convective stratiform precipitation (Gallus, 1999).

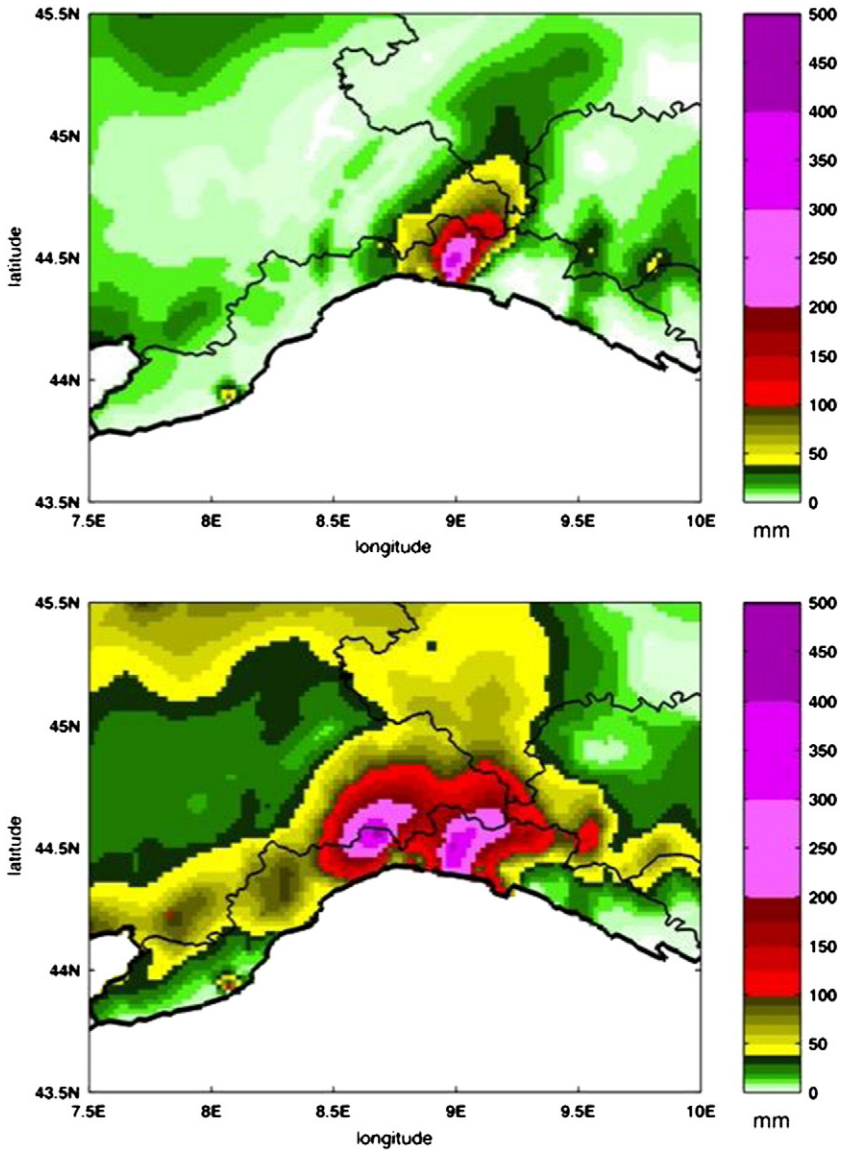

Fig. 6. Rainfall depth between 09UTC and 15UTC (upper panel) and daily total accumulation (lower panel) on November 4th 2011, as observed by the ICPD raingauge network. (No data on the sea is due to the absence of observations).

Having clearly in mind the uncertainty and limitation of the microphysics scheme and the explicit/parameterized cumulus convection, we took the decision to run quite an extensive numerical experiment.

Initial and boundary conditions for the hindcast model experiments shown here are provided by the European Centre for Medium-Range Weather Forecast (ECMWF Integrated Forecast System IFS) at 0.125° (about 16 km). The time of initialization for the first 10 simulations (Table 1) was on November 3rd 2011 at 12 UTC. Land surface and SST fields were as well initialized with ECMWF products on November 3rd 2011 at 12 UTC (not shown). Some experiments were also performed with GFS analysis a 0.5° (about 60 km), but the results were not good enough to justify further investigations (not shown here).

4. Analysis of the modeling results

4.1. The role of convective parameterization

The first part of this section focuses on evaluation of the QPF products provided by the first 10 experiments on the nested domain d_2 and covering the time window from 09UTC to 15 UTC (Fig. 8). All ten-model configurations underestimate the observed rainfall depth (Fig. 9, middle line-central panel) obtained by rain gauge analyses. They show a 'localization error' in spatial displacement of the event on the order of 20–25 km to the west. These deficiencies are directly related to differences in the fine-scale spatio-temporal features between the forecasted and observed convective cell responsible for the event. One principle issue is that in nature, by the fact that the

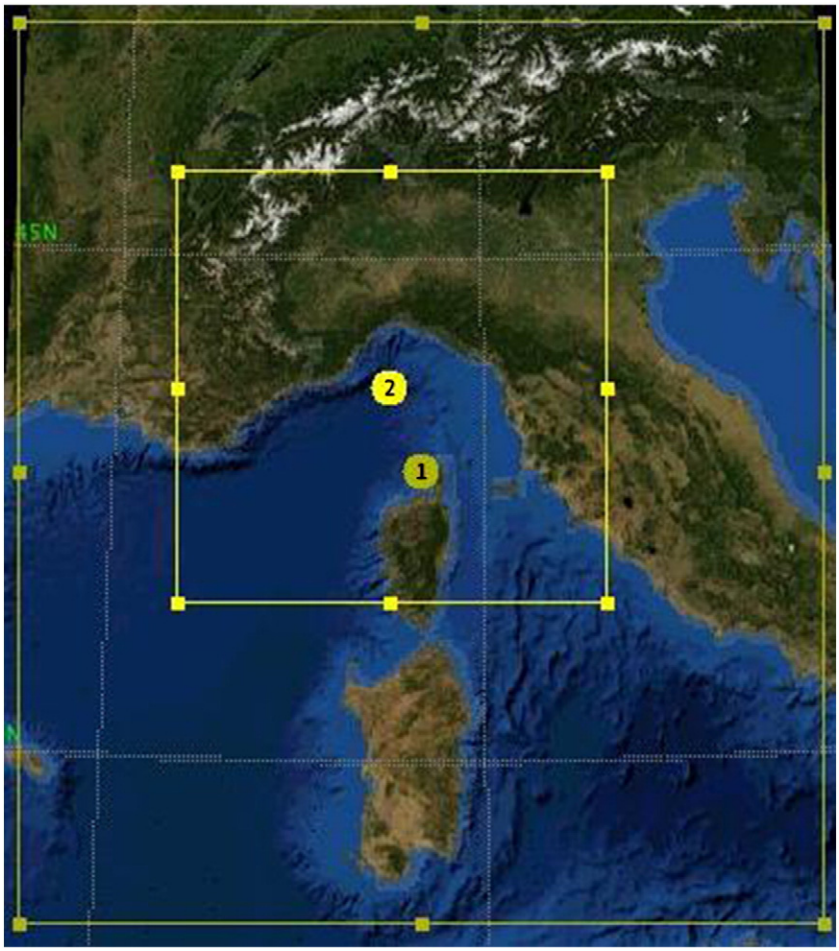

Fig. 7. Domains d_1 (dx = dy = 5 km) and d_2 (dx = dy = 1 km) adopted for WRF simulations.

triggering location is contained in a very small region, like a finger (Rebora et al., 2013), the total cell width ranges from 5 to 10 km. Such fine-scale structure is challenging for most NWP models operating on the order of 1 km grid spacing. Second, while the observed convective cell exhibited a characteristic v-shape and a general persistence over the Genoa city area, both explicit and parameterized convection model simulations in the 1 km nested domain result in excessively widespread convection covering most of the central part of the Liguria Apennines for the 10 simulations initialized on November 3rd. This common behavior among the experiments suggests a general deficiency of the model, but also of the mesoscale dynamic processes of the parent model, in reproducing the precise location of prominent local, low-level convergence responsible for the persistence of the cell over the city of Genoa and surrounding terrain.

Table 1
microphysics and cumulus convection parameterization settings adopted over domain d_1 (5 km grid spacing) and d_2 (1 km grid spacing).

Member	Cumulus scheme d_1	Cumulus scheme d_2	Microphysics
KF-KF-W	Kain–Fritsch	Kain–Fritsch	WSM6
KF-KF-T	Kain–Fritsch	Kain–Fritsch	Thompson
BMJ-BMJ-W	Betts–Miller–Janijc	Betts–Miller–Janijc	WSM6
BMJ-BMJ-T	Betts–Miller–Janijc	Betts–Miller–Janijc	Thompson
KW-E-W	Kain–Fritsch	Explicit	WSM6
KW-E-T	Kain–Fritsch	Explicit	Thompson
BMJ-E-W	Betts–Miller–Janijc	Explicit	WSM6
BMJ-E-T	Betts–Miller–Janijc	Explicit	Thompson
E-E-W	Explicit	Explicit	WSM6
E-E-T	Explicit	Explicit	Thompson

The 24 h QPFs from November 4th 00UTC to November 5th 00UTC (not shown for sake of conciseness) produce a prediction slightly more consistent with the observed one. This result suggests to focalize the attention on the role of microphysics in this extreme event since convection seams not to be so discriminate to drive the process. On the basis of this consideration, the Mean Absolute Error (MAE) has been computed by using the nearest model grid points to the Liguria region rainguage stations available within the d_2 domain. The values in Table 2 suggest that, for prescribed microphysics, the lower MAEs are obtained for both of fully explicit runs E-E-W and E-E-T. Each one of the two runs in fact is slightly outperform the other settings at fixed microphysics since the E-E-W with respect to the BMJ-E-W or the KF-E-W and the E-E-T with respect to the BMJ-BMJ-T.

On the basis of the preliminary results on the QPF analysis, a second set of experiments was conducted to explore the

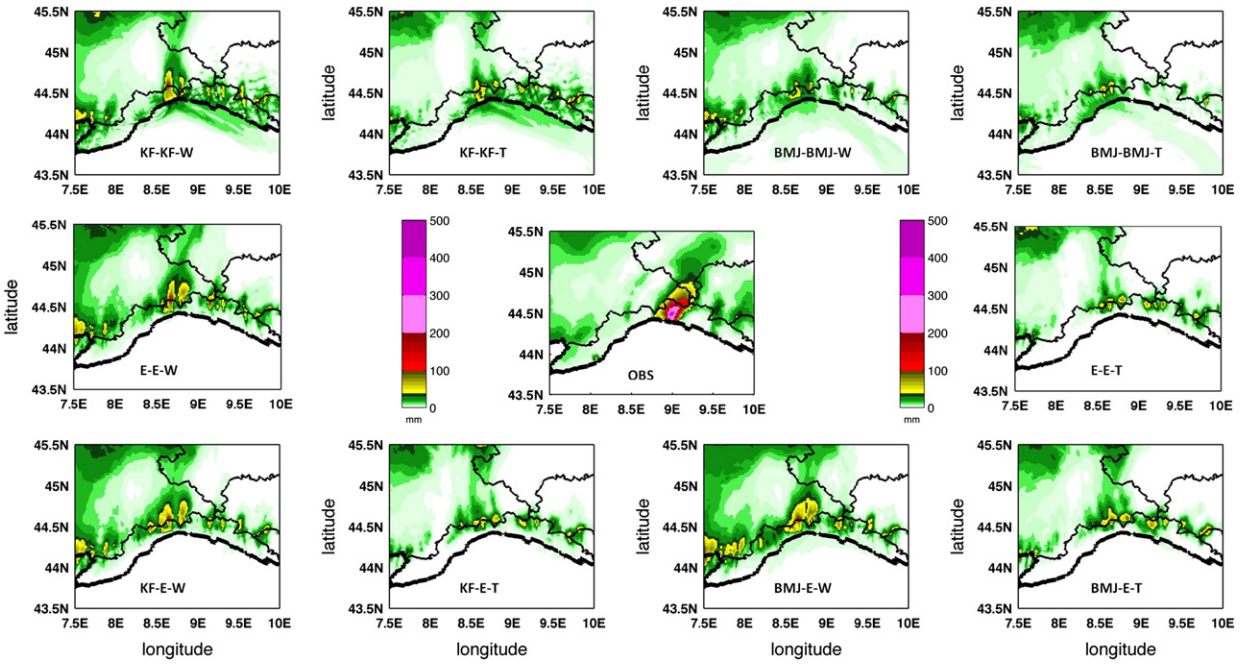

Fig. 8. Rainfall depth (color code mm/6 h) from 09UTC to 15UTC on November 4th 2011. First line from left to right: KF-KF-W, KF-KF-T, BMJ-BMJ-W, BMJ-BMJ-T. Middle line: from left to right E-E-W, observed rainfall depth, E-E-T. Third line from left to right: KF-E-W, KF-E-T, BMJ-E-W, BMJ-E-T.

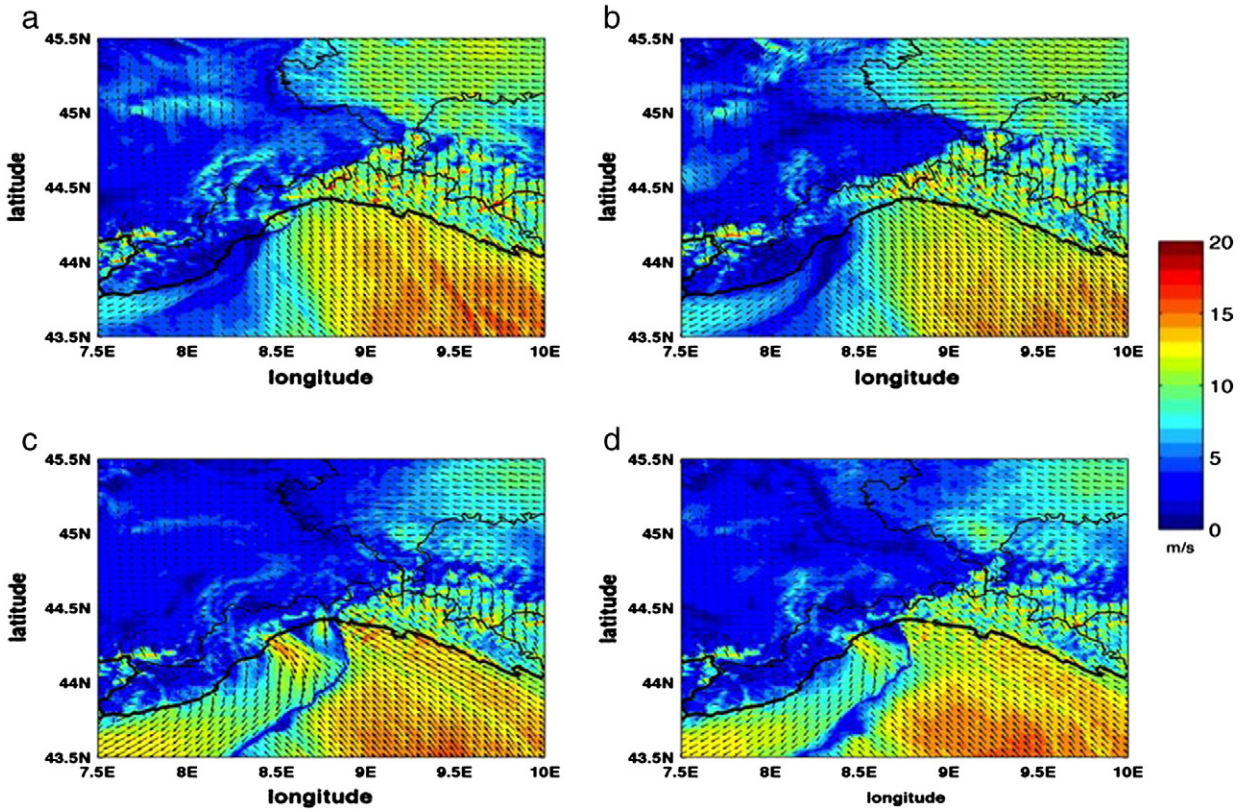

Fig. 9. Wind field prediction at 10 m on November 4th, at 12 UTC, 1 km grid spacing. Panels a) and b) refer to E-E-W and E-E-T settings (28 vertical levels), with IC and BC from IFS model—November 3rd 12 UTC. Panels c) and d) refer to E-E-W and E-E-T settings (28 vertical levels), with IC and BC from IFS model—November 4th 00UTC.

Table 2
Mean Absolute Error (MAE) for the ten modelsettings (24 hour rainfall depth at Liguria region raingauge stations).

Member	MAE [mm]
KF-KF-W	62.9
KF-KF-T	63.8
BMJ-BMJ-W	78.7
BMJ-BMJ-T	62.7
KF-E-W	61.0
KF-E-T	63.4
BMJ-E-W	56.7
BMJ-E-T	63.5
E-E-W	56.5
E-E-T	62.5

potential lead time horizon for capturing significant features of this event. Only the E-E-W and E-E-T were used as physical processes configurations with ICs and BCs provided by ECMWF-IFS. Both runs were initialized on November 4th at 00UTC (as opposed to 12 UTC Nov.3rd) in order to assess the sensitivity of the forecast to the initialization time.

The main improvement in re-running these two configurations with atmospheric conditions closer in time to the event is shown in Fig. 9. The forecasted wind field at 10 m for the E-E-W and E-E-T configurations (Fig. 9a and b, at 12 UTC) initialized on November 3rd at 12 UTC is compared with the new predicted wind field at 10 m (panels c and d) for the E-E-W and E-E-T configurations. The striking result is that, the convergence line highlighted by ASCAT observations (Fig. 5), is not well represented in terms of spatial location and intensity in both cases initialized on November 3rd, 12 UTC. In particular, in the E-E-T simulation the strongest contribution from the northwest low-level jet is not equally balanced by the south-east warmer counterpart. On the contrary, in the E-E-W case (panel a) the south–east low level flow is more intense than in E-E-T case but the cold and dry counterpart coming from the orography is not sufficiently strong to generate a line of convergence. The model is able to capture the convergence line in both new runs (Fig. 9 panels c and d). With model initialization on November 3rd at 12UTC (Fig. 9a and b) the wind coming from the south–east is quite excessive and appears to potentially force a major quantity of precipitation over the west side of the Liguria

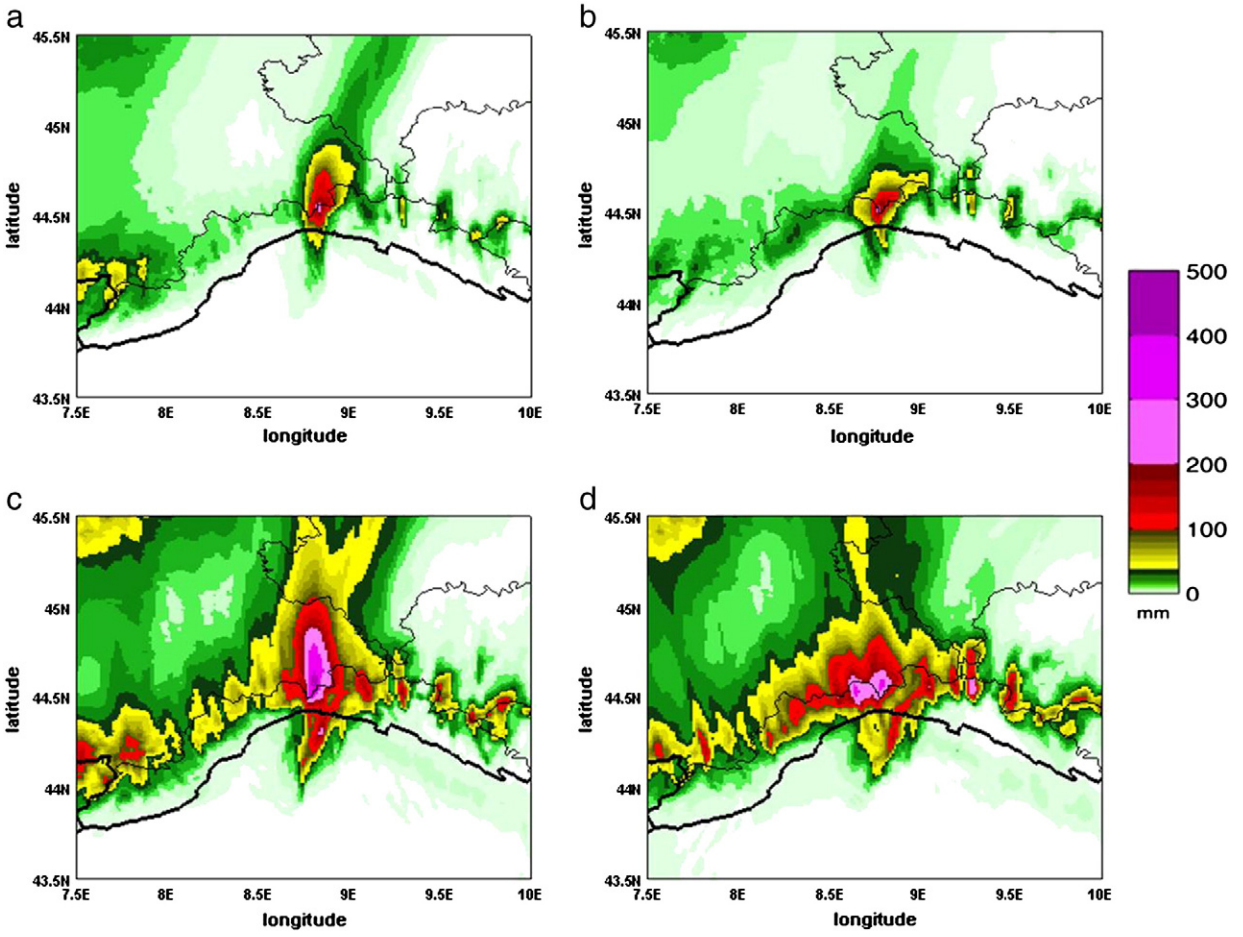

Fig. 10. QPF on November 4th, 1 km grid spacing, 28 vertical levels, IC and BC from IFS model (run on November 4th 00UTC). First line: QPF 09–15 UTC on November 4th with panels a) E-E-W and b) E-E-T settings. Second line: daily QPF on November 4th with panels c) E-E-W and d) E-E-T settings.

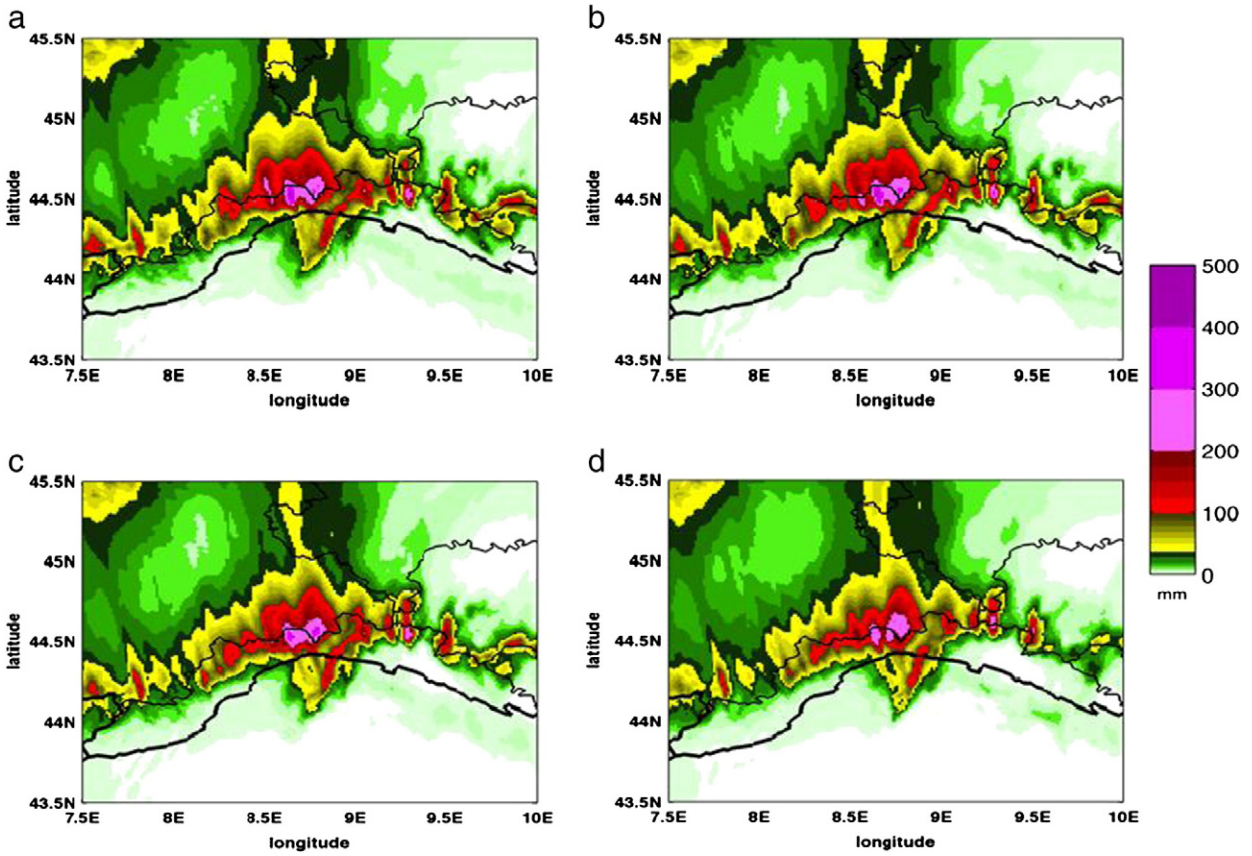

Fig. 11. QPF on November 4th, 0-24UTC, 1 km grid spacing, E-E-T setup with 84 vertical levels and IC and BC from IFS model—November 4th 00UTC. Panels a) refers to $Nt_C = 25 * 10^6\ m^{-3}$, b) to $Nt_C = 50 * 10^6\ m^{-3}$, c) to $Nt_C = 100 * 10^6\ m^{-3}$, and d) to $Nt_C = 500 * 10^6\ m^{-3}$.

region (Fig. 8). In the 00UTC initialization, strong convergence is now possible since the Sirocco wind, which blows hot and moist air through the region, is better balanced by a stronger northerly low-level jet, which transports cold air towards the Genoa area. The presence of this northerly component in the wind field supports the development of a quasi-stationary v-shaped re-generating convective storm system which is similar to the one depicted in Rebora et al. 2013.

The effects of running different initializations are also evident comparing the QPFs from 09UTC to 15UTC. The E-E-W and E-E-T configurations initialized on November 4th at 00UTC (Fig. 10a and b) now exhibit a pattern more similar to the observed event (Fig. 6, upper panel) in terms of precipitation depth in the Genoa area compared to the previous runs initialized twelve hours before (Fig. 8, middle line right and left panel respectively). In terms of the spatial representation of the precipitation pattern, the Thomson microphysics evolves a QPF pattern more similar to the observed pattern (i.e. the double maximum in the daily precipitation). Thus, at this stage of the study, the results suggest the E-E-T configuration is deemed to be modestly better.

4.2. Microphysical influences on the pattern of precipitation

Until this point attention was focused on the role of convective representation in the model forecasts and the results have suggested that the explicit treatment of this process produces somewhat better forecasts. On the basis of these results, a third set of analyses have been conducted to evaluate the sensitivity of the model to different values of microphysical parameters. Specifically, the prescribed number of initial cloud droplets Nt_c created upon autoconversion of water vapor to cloud water in the Thompson microphysics was evaluated. Based on observational data, Nt_c usually falls in the range of $25–100 * 10^6\ m^{-3}$ for maritime rainfall cases, while values around $300–500 * 10^6\ m^{-3}$ are recommended for continental ones (Thompson et al., 2008). The two initial sets of E-E-T experiments used a default Nt_c value equal to $100 * 10^6\ m^{-3}$. Three additional experiments were then performed setting Nt_c respectively equal to $25 * 10^6$ and $50 * 10^6\ m^{-3}$ (extreme maritime cases), and $Nt_c = 500 * 10^6\ m^{-3}$, to represent a more continental airmass. Moreover, for this specific set of experiments the vertical levels were increased from 28 to 84 to better capture the low-level circulation and the dynamics over the complex topography of this area.

Fig. 12. Horizontal sections of horizontal wind field prediction (shaded map represents the wind speed, the arrows represents the wind direction) at 10 m on November 4th, 1 km grid spacing, E-E-T setup with 84 vertical levels, IC and BC from IFS model—November 4th 00 UTC, $Nt_C = 25 * 10^6\ m^{-3}$. Panels refers a) at 06UTC, b) at 09UTC, c) at 12UTC.

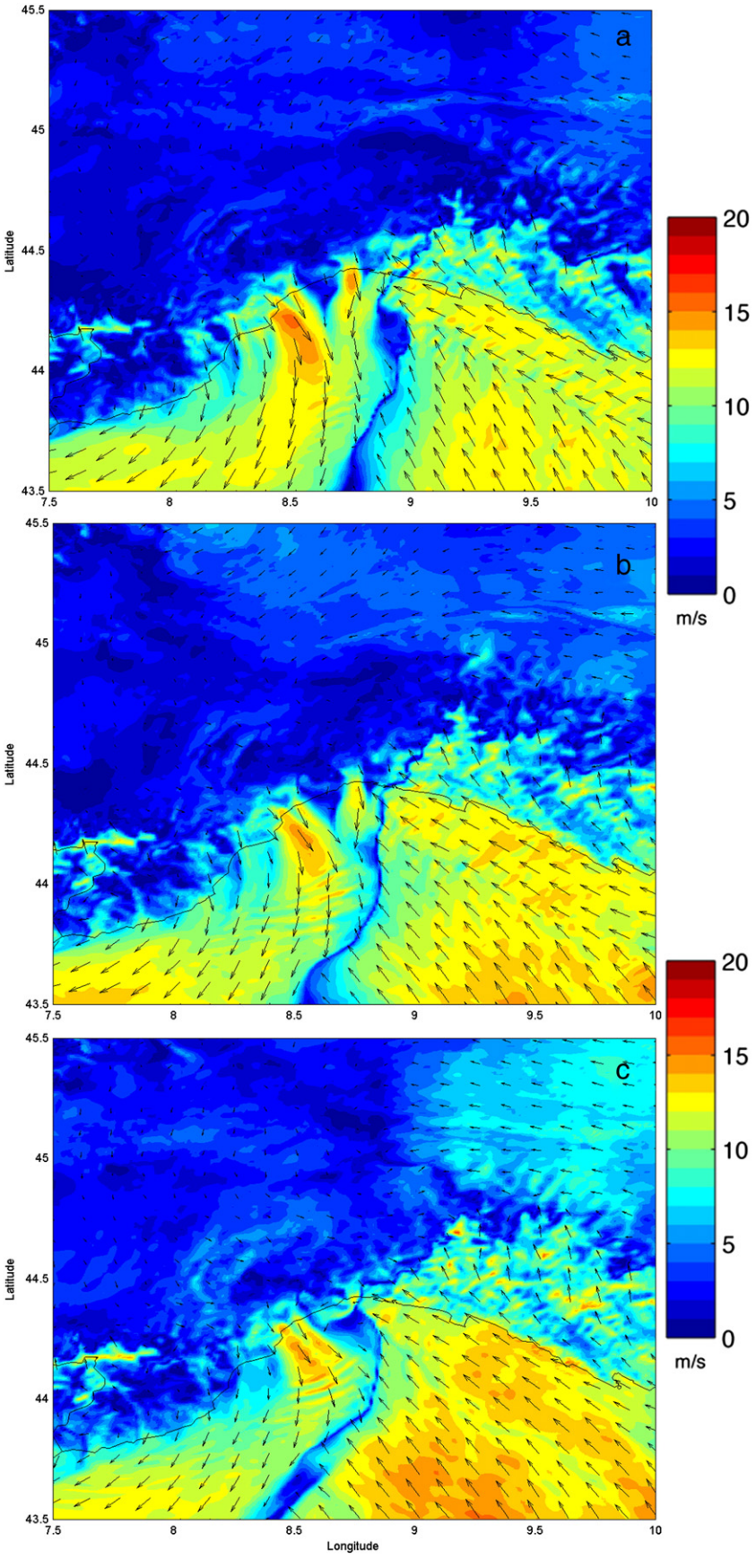
a
b
c
Latitude
Longitude
45.5
45
44.5
44
43.5
7.5
8
8.5
9
9.5
10
20
15
10
5
0
m/s

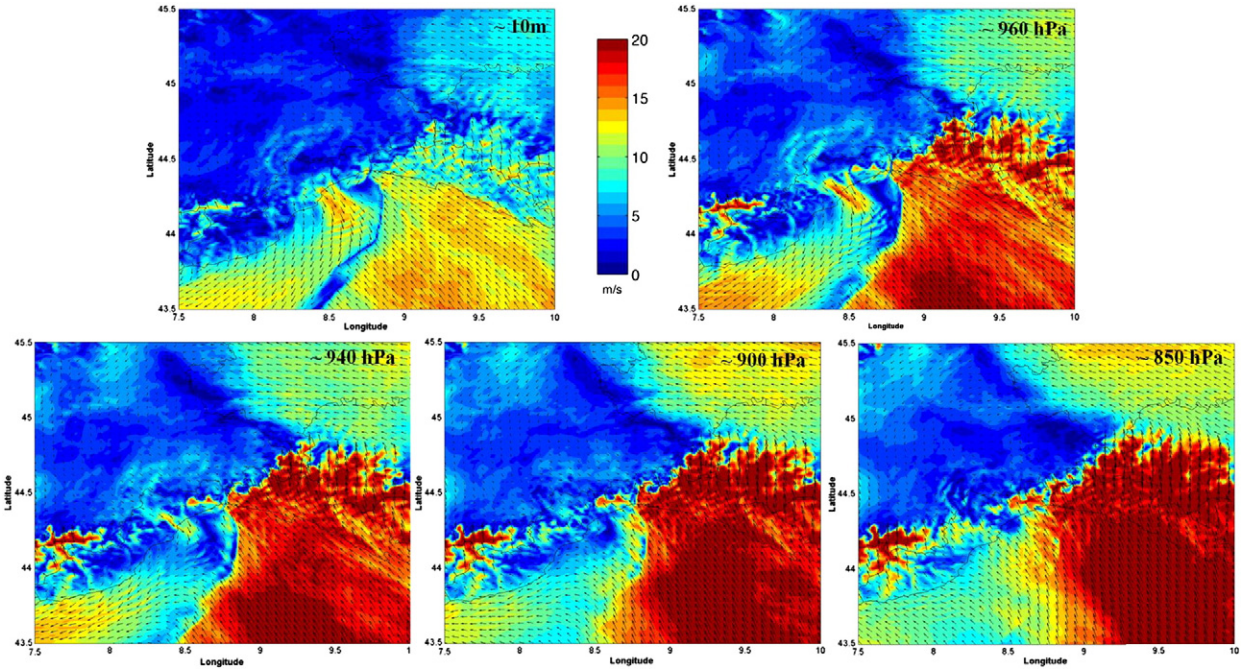

Fig. 13. Horizontal sections of horizontal wind speed prediction (shaded map represents the wind speed, the arrows represents the wind direction) along the Ligurian coastline on November 4th at 12 UTC at five different elevations: 10 m, ~960 hPa, ~940 hPa, ~900 hPa and ~850 hPa. E-E-T setup, 1 km grid spacing and 84 vertical levels, IC and BC from IFS model — November 4th 00 UTC-$Nt_C = 25 * 10^6\ m^{-3}$.

In the 24 h QPF maps resulting from these last four experiments (Fig. 11), the overall rainfall pattern does not change significantly moving from the extreme maritime cases to the continental ones. Conversely, differences do arise in the values for the 24 h peak rainfall depth. There is a direct relationship between the value of Nt_c used and the peak rainfall amounts. A more maritime value of $Nt_c = 25 * 10^6$ and $50 * 10^6\ m^{-3}$ produces around 420–425 mm/24 h of peak rainfall, while only around 350 and 280 mm/24 h are produced for $Nt_c = 100$ and $500 * 10^6\ m^{-3}$, respectively. This result confirms that a proper setting of the prescribed number of initial cloud droplets Nt_c, reflecting the observed characteristics of the extreme event under examination, provides useful guidance in these numerical experiments. It also leads to a significant improvement of the QPF with respect to the previous simulations not only in terms of the value of peak rainfall but also in the spatial pattern. In fact at this point of the work the heavy rainfalls that hit the central-west and central-east area of Genoa (Fig. 6, lower panel) are now captured by the simulations.

The reason for the lower than observed rainfall values on the right, (eastern) main convective cell over the central-eastern Liguria is further explored by analyzing the model E-E-T wind fields both at the surface (Fig. 12) and at different pressure levels at 12UTC (Fig. 13). The three panels in Fig. 12 are the wind field with Nt_c equal to $25 * 10^6\ m^{-3}$on November 4th at 06UTC, 09UTC and 12UTC, respectively. Moving from 06UTC (panel a) to 12 UTC (panel c), the model shows the Sirocco (southeasterly) wind increases in time more than the northerly low-level jet. This difference in the two wind components of the line of converge appears to reduce the balance between the two and results in a rapid movement of the line of convergence towards the central-western Liguria. This quick change in the position of the convergence line in turn reduces the peak value of the QPF over the central-eastern Liguria.

The five panels in Fig. 13 show the model wind field on November 4th at 12UTC at five different heights: 10 m, ~960 hPa, ~940 hPa, ~900 and ~850 hPa. Fig. 13 shows that, from one side, the Sirocco wind tends to increase in intensity with the elevation. On the other side, the northerly low-level jet active at the lower level does not preserve its intensity with elevation. This situation results in the three-dimensional convergence surface becoming unstable and shifting to West. However, observed wind data do not support such a rapid shifting of the convergence surface. Fig. 14 shows the near surface wind observations nearest to the convergence region compared to the modeled wind in the same positions. It is evident that the model evolves a Sirocco wind stronger than the observed one. The ground truth observations are instead consistent with the stability of the convergence surface and so with higher rainfall observation on the central-eastern Genoa hills.

It is interesting to note that several intense waterspouts were observed during the day of the event off the Genoa coastline by local stormchasers (Fig. 15). The phenomena, active on the micro-β scale (20–200 m, Orlanski, 1975), were enhanced by the intense vorticity generation along the convergence surface and by the appreciable low-level horizontal wind shear.

The previous considerations suggest that the inability of the WRF model to capture the low level wind field at meso-γ scale inhibits a proper representation of the detailed spatial

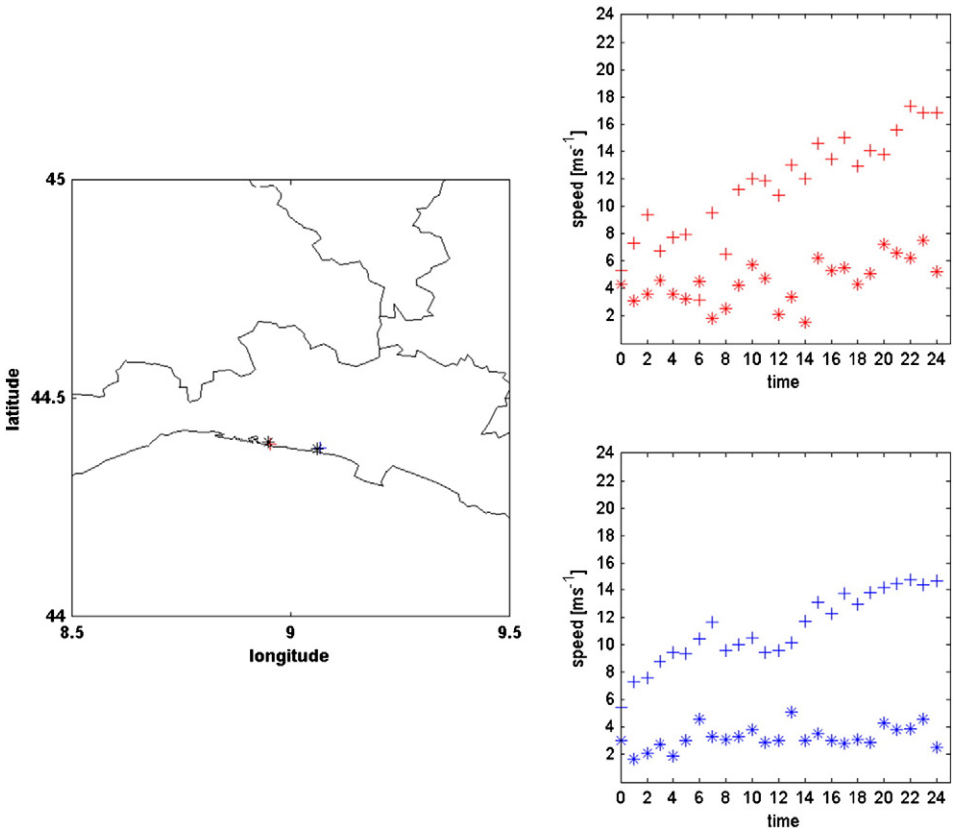

Fig. 14. Wind speed at 10 m on November 4th, 0–24 UTC. (*) represent the time series observed by the ICPD raingauge network working during the extreme event. (+) represent the time series forecast by the E-E-T setup with 1 km grid spacing with 84 vertical levels, IC and BC from IFS model—November 4th 00 UTC, $Nt_C = 25 * 10^6\ m^{-3}$.

Fig. 15. Tornadic waterspouts on November 4th 2011, ~20 km off shore SE-S of Genoa (courtesy of N. Ubalducci storm chaser, 2011 personal communication).

and temporal structure of the convergence line and the consequent rainfall at the ground.

5. Discussion and conclusions

This paper has analyzed the physical conditions that led to the catastrophic flash flood event that took place in Genoa, Italy during the mid-day hours of November 4th 2011. Model forecast experiments using a selection of cumulus convection and microphysical parameterizations in the ARW-WRF modeling system were conducted with the intention of recreating the natural storm event as observed from different platforms such as raingauges, radiosondes and ASCAT spaceborne scatterometer estimated wind fields.

The extreme, >200 yr return period, event was characterized by the typical ingredients leading to heavy rainfall and flash flooding, such as an unstable airmass, a moist low-level jet, the presence of orography orthogonal to the flow and a slowly-evolving synoptic pattern. The fact that existing operational high-resolution model runs were unable to capture the location and magnitude of the event prompted this detailed study and the different set of WRF model hindcast experiments where both implicit and explicit convection schemes were adopted in the convection permitting scale range. The two two-way nested integration domains used in the numerical simulations have fixed horizontal resolutions of 5 km and 1 km respectively.

While selections of grid spacings, cloud microphysics and convective closure methodologies all imparted sensitivities to the model hindcasts, the biggest improvement was found when the time of initialization was moved much closer to the event, even though no formal data assimilation scheme was used. This result suggests that either the longer-lead initialization lacked all the proper characteristics of the observed conditions at that time, or that the WRF model was simply unable to properly evolve the necessary mesoscale features required to trigger this long-lived event. While it is certainly true that the WRF model possesses error structures that may inhibit it to generate an event at long lead-times, the fact that it was able to predict a very representative type of event suggests that the IFS analysis on November 3rd at 12UTC may have been the principle cause of the deficiency. Given the relatively coarse scale of the IFS analysis, it is certainly possible that the specific thermodynamic or circulation features, which ultimately evolved into the Genoa event, may have been unresolved. Without additional data it will be difficult to definitively assess the reason for the relative failure of the 12z initialization.

Only meso-γ details of the event where not completely captured by the best setting of the ARW-WRF model. That is the reason why peak hourly rainfalls were not perfectly reproduced.

The selection of explicit treatment of convection on both domains and a higher number of vertical levels especially in the boundary layer had a positive impact on not only the total value of QPF for the entire day of the event but also in terms of spatial distribution of the precipitation field. Also, considered adjustment of microphysics parameters, specifically the auto-conversion initial drop size concentration resulted in an overall improvement of the model forecasts. In the case of this extreme Mediterranean storm event, the values which produced superior precipitation intensity results were in fact more reflective of a maritime environment.

Lastly, in onging work, we are investigating the capability of a fully-coupled NWP-distributed hydrological model to predict various hydrometeorological aspects of the 4th November 2011 event. The purpose of this exercise is two-fold in that we seek to determine a) whether or not there is any sensitivity in land surface initial conditions which may significantly impact this event and b) what the potential lead time for flash flood guidance from this system may be for these kinds of events. Given the strong synoptic scale and mesoscale dynamical forcing conditions and the existence of widespread cloud cover over much of the internal domain, the influence of the land surface initialization is hypothesized to be minimal. However, the potential of providing longer lead-time on flash flood guidance through the use of a single unified modeling system would certainly have significant value. Because the WRF model has demonstrated some relative skill in predicting important features of this event in a true hindcast mode there is the potential to add up to 5–6 h more lead time, accounting for model integration time, to regional flash flood forecasts, for these kinds of events.

Acknowledgments

This work is supported by the Italian Civil Protection Department and by the Regione Liguria. We acknowledge Regione Liguria and Regione Piemonte for providing us with the data of the regional meteorological observation networks. We acknowledge the Italian Civil Protection Department for providing us with the Italian Radar Network data. We are very grateful to the meteorologists and the hydrologists of the Meteo-Hydrologic Centre of Liguria Region, as well as to Greg Thompson (NCAR) for many useful discussions. The portion of work carried out by Simone Tanelli was performed at Jet Propulsion Laboratory, California Institute of Technology, under contract with the National Aeronautics and Space Administration; likewise, support from the Precipitation Measurement Mission program is gratefully acknowledged. Elisabetta Fiori, Nicola Rebora and Antonio Parodi would like to acknowledge the support of the FP7 DRIHM (Distributed Research Infrastructure for Hydro-Meteorology, 2011-2015) project (contract number 283568). David J. Gochis is supported by the National Center for Atmospheric Research (NCAR). NCAR is supported by a cooperative grant from the U.S. National Science Foundation (NSF). Gochis also acknowledges support for this project from NSF Grant OCI-1234742. The numerical simulations were performed on the SuperMUC Petascale System of the LRZ Supercomputing Centre, Garching, Germany. Project-ID: pr45de.

References

Altinbilek, D., Barret, E.C., Oweis, T., Salameh, E., Siccardi, F., 1997. Rainfall climatology on the Mediterranean, EU-AVI 080 Project ACROSS—analyzed climatology rainfall obtained from satellite and surface data in the Mediterranean basin. EC reports.

Arakawa, Akio, 2004. The cumulus parameterization problem: past, present, and future. J. Clim. 17, 2493–2525. http://dx.doi.org/10.1175/1520-0442(2004)017<2493:RATCPP>2.0.CO;2.

Argence, S., Lambert, D., Richard, E., Chaboureau, J.-P., Söhne, N., 2008. Impact of initial condition uncertainties on the predictability of heavy rainfall in the Mediterranean: a case study. Q. J. R. Meteorol. Soc. 134, 1775–1788. http://dx.doi.org/10.1002/qj.314.

Barredo, J.I., 2007. Major flood disasters in Europe: 1950–2005. Nat. Hazards 42, 125–148.

Betts, A.K., 1986. A new convective adjustment scheme. Part I: Observational and theoretical basis. Q. J. R. Meteorol. Soc. 112, 677–691.

Betts, A.K., Miller, M.J., 1986. A new convective adjustment scheme. Part II: Single column tests using GATE wave, BOMEX, ATEX and arctic air-mass data sets. Q. J. R. Meteorol. Soc. 112, 693–709.

Boni, G., Parodi, A., Rudari, R., 2006. Extreme rainfall events: learning from raingauge time series. J. Hydrol. 327, 304–314.

Boni, G., Parodi, A., Siccardi, F., 2008. A new parsimonious methodology of mapping the spatial variability of annual maximum rainfall in mountainous environments. J. Hydrometeorol. 9, 492–506. http://dx.doi.org/10.1175/2007JHM900.1.

Borga, M., Boscolo, P., Zanon, F., Sangati, M., 2007. Hydrometeorological analysis of the August 29, 2003 flash flood in the eastern Italian Alps. J. Hydrometeorol. 8 (5), 1049–1067.

Branković, Č., Matjačić, B., Ivatek-Šahdan, S., Buizza, R., 2008. Downscaling of ECMWF ensemble forecasts for cases of severe weather: ensemble statistics and cluster analysis. Mon. Weather Rev. 136 (9), 3323–3342.

Chappell, C.F., 1986. Quasi-stationary convective events. Mesoscale meteorology and forecasting. In: Ray, P.S. (Ed.), Am. Meteorol. Soc. 289–310.

Delrieu, Guy, Nicol, John, Yates, Eddy, Kirstetter, Pierre-Emmanuel, Creutin, Jean-Dominique, Anquetin, Sandrine, Obled, Charles, Saulnier, Georges-Marie, 2005. The catastrophic flash-flood event of 8–9 September 2002 in the Gard Region, France: a first case study for the Cévennes–Vivarais Mediterranean Hydrometeorological Observatory. J. Hydrometeorol. 6, 34–52.

Done, J., Davis, C.A., Weisman, M., 2004. The next generation of NWP: explicit forecasts of convection using the weather research and forecasting (WRF) model. Atmos. Sci. Lett. 5, 110–117.

Doswell, C.A., Ramis, C., Romero, R., Alonso, S., 1998. A diagnostic study of three heavy precipitation episodes in the Western Mediterranean region. Weather Forecast. 13, 102–124.

Droegemeier, K.K., 1997. The numerical prediction of thunderstorms: challenges, potential benefits, and results from realtime operational tests. WMO Bull. 46, 324–336.
Ducrocq, V., Nuissier, O., Ricard, D., Lebeaupin, C., Thouvenin, T., 2008. A numerical study of three catastrophic precipitating events over western mediterranean region (Southern France): Part II: Mesoscale triggering ans stationarity factors. Q. J. R. Meteorol. Soc. 134 (630), 131–145.
Dudhia, J., Hong, S.-Y., Lim, K.-S., 2008. A new unified mixed-phase particle fall speed in bulk microphysics parameterizations. 9th WRF Users' Workshop, Boulder CO, June 2008.
Gallus, William A., 1999. Eta simulations of three extreme precipitation events: sensitivity to resolution and convective parameterization. Weather Forecast. 14, 405–426.
Gerard, L., 2007. An integrated package for subgrid convection, clouds and precipitation compatible with meso-gamma scales. Q. J. R. Meteorol. Soc. 133, 711–730.
Groisman, Pavel Ya, Knight, R.W., Karl, T.R., Easterling, D.R., Sun, B., Lawrimore, J.M., 2004. Contemporary changes of the hydrological cycle over the contiguous United States: trends derived from in situ observations. J. Hydrometeorol. 5, 64–85.
Groisman, Pavel Ya, Knight, Richard W., Easterling, David R., Karl, Thomas R., Hegerl, Gabriele C., Razuvaev, Vyacheslav N., 2005. Trends in intense precipitation in the climate record. J. Climate 18, 1326–1350.
Hong, S.Y., Lim, J.O.J., 2006. The WRF single moment 6-class microphysics scheme (WSM6). J. Korean Meteorol. Soc. 42, 129–151.
Hong, S.-Y., Dudhia, J., Chen, S.-H., 2004. A revised approach to ice-microphysical processes for the bulk parameterization of cloud and precipitation. Mon. Weather Rev. 132, 103–120.
Jankov, I., Gallus, W., Segal, M., Shaw, B., Koch, S., 2005. The impact of different WRF model physical parameterizations and their interactions on warm season MCS rainfall. Weather Forecast. 20, 1048–1060.
Kain, J.S., Fritsch, M., 1990. A one-dimensional entraining/detraining plume model and its application in convective parameterization. J. Atmos. Sci. 47, 2784–2802.
Kain, J.S., Weiss, S.J., Levit, J.J., Baldwin, M.E., Bright, D.R., 2006. Examination of convection-allowing configurations of the WRF model for the prediction of severe convective weather: the SPC/NSSL Spring Program 2004. Weather Forecast. 21, 167–181. http://dx.doi.org/10.1175/WAF906.1.
Kain, J.S., Weiss, S.J., Bright, D.R., Baldwin, M.E., Levit, J.J., Carbin, G.W., Schwartz, C.S., Weisman, M.L., Droegemeier, K.K., Weber, D.B., Thomas, K.W., 2008. Some practical considerations regarding horizontal resolution in the first generation of operational convection-allowing NWP. Weather Forecast. 23, 931–952.
Komuscu, A.U., Erkan, A., Celik, S., 1998. Analysis of the meteorological and terrain features leading to the Izmir flash flood. Nat. Hazards 18, 1–25.
Lilly, D.K., 1990. Numerical prediction of thunderstorms—has its time come? Q. J. R. Meteorol. Soc. 116 (494), 779–798.
Lin, Y.-L., Farley, Richard D., Orville, Harold D., 1983. Bulk parameterization of the snow field in a cloud model. J. Clim. Appl. Meteorol. 22, 1065–1092.
Lin, L.-Y., Chiao, S., Wang, T., Kaplan, M.L., Weglarz, R.P., 2001. Some common ingredients for heavy orographic rainfall. Weather Forecast. 16, 633–660.
Llasat, M.C., Barriendos, M., Rigo, T., 2003. The "Montserrat-2000" flash-flood event: a comparison with the floods that have occurred in the Northeast Iberian Peninsula since the 14th Century. Int. J. Climatol. 23, 453–469.
Llasat-Botija, M., Llasat, M.C., López, L., 2007. Natural hazards and the press in the western Mediterranean region. Adv. Geosci. 12, 81–85.
Massacand, A.C., Wernli, H., Davies, H.C., 1998. Heavy precipitation on the alpine southside: an upper-level precursor. Geophys. Res. Lett. 25 (9), 1435–1438.
Miglietta, M.M., Rotunno, R., 2010. Numerical simulations of low-CAPE flows over a mountain ridge. J. Atmos. Sci. 67, 2391–2401. http://dx.doi.org/10.1175/2010JAS3378.1.
Molini, L., Parodi, A., Rebora, N., Craig, G.C., 2011. Classifying severe rainfall events over Italy by hydrometeorological and dynamical criteria. Q. J. R. Meteorol. Soc. 137, 148–154.
Moncrieff, M.W., Liu, C., 1999. Convection initiation by density currents: role of convergence, shear, and dynamical organization. Mon. Weather Rev. 127, 2455–2464.
Orlanski, I., 1975. A rational subdivision of scales for atmospheric processes. Bull. Am. Meteorol. Soc. 56, 527–530.
Parodi, A., Boni, G., Ferraris, L., Siccardi, F., Pagliara, P., Trovatore, E., Foufoula-Georgiou, E., Kranzlmueller, D., 2012. The "perfect storm": from across the Atlantic to the hills of Genoa. EOS 93 (24).
Rebora, N., Molini, L., Casella, E., Comellas, A., Fiori, E., Pignone, F., Siccardi, F., Silvestro, F., Tanelli, S., Parodi, A., 2013. Extreme rainfall in the Mediterranean: what can we learn from observations? J. Hydrometeorol. 14, 906–922.
Ricard, Didier, Ducrocq, Véronique, Auger, Ludovic, 2012. A climatology of the mesoscale environment associated with heavily precipitating events over a northwestern Mediterranean area. J. Appl. Meteorol. Climatol. 51, 468–488. http://dx.doi.org/10.1175/JAMC-D-11-017.1.
Roberts, N.M., Lean, Humphrey W., 2008. Scale-selective verification of rainfall accumulations from high-resolution forecasts of convective events. Mon. Weather Rev. 136, 78–97. http://dx.doi.org/10.1175/2007MWR2123.1.
Roth, G., La Barbera, P., Greco, M., 1996. On the description of the basin drainage structure. J. Hydrol. 187, 119–135.
Siccardi, F., 1996. Rainstorm hazards and related disasters in the western Mediterranean region. Remote Sens. Rev. 14, 5–21.
Skamarock, W.C., Klemp, J.B., Dudhia, J., Gill, D.O., Barker, D.M., Wang, W., Powers, J.G., 2005. A description of the Advanced Research WRF version 2. NCAR Tech. Note NCAR/TN-468 + STR (88 pp.).
Thompson, G., Rasmussen, R.M., Manning, K., 2004. Explicit Forecasts of winter precipitation using an improved bulk microphysics scheme. Part I: Description and sensitivity analysis. Mon. Weather Rev. 132, 519–542.
Thompson, G., Field, P.R., Rasmussen, R.M., Hall, W.D., 2008. Explicit forecasts of winter precipitation using an improved bulk microphysics scheme. Part II: Implementation of a new snow parameterization. Mon. Weather Rev. 136, 5095–5115.
Tripoli, G.J., Medaglia, C.M., Dietrich, S., Mugnai, A., Panegrossi, G., Pinori, S., Smith, E.A., 2005. The 9–10 November 2001 Algerian flood. Bull. Am. Meteorol. Soc. 86, 1229–1235.
Wang, Jian-Jian, Rauber, Robert M., Ochs, Harry T., Carbone, Richard E., 2000. The effects of the island of Hawaii on offshore rainband evolution. Mon. Weather Rev. 128, 1052–1069.
Xue, M., Droegemeier, K.K., Weber, D., 2007. Numerical prediction of high-impact local weather: a driver for petascale computing. Petascale Computing: Algorithms and Applications.LLC 103–124.
Yu, X., Lee, T.-Y., 2010. Role of convective parameterization in simulations of a convection band at grey-zone resolutions. Tellus 62A, 617–632.